Properties of strange quark matter under strong rotation

Fei Sun[1,2,4,*] and Anping Huang[2,3,†]

[1]*Department of Physics, China Three Gorges University, Yichang, 443002, China*
[2]*Physics Department and Center for Exploration of Energy and Matter, Indiana University, 2401 N Milo B. Sampson Lane, Bloomington, Indiana 47408, USA*
[3]*School of Nuclear Science and Technology, University of Chinese Academy of Sciences, Beijing 100049, China*
[4]*Center for Astronomy and Space Sciences, China Three Gorges University, Yichang 443002, China*

(Received 30 June 2021; revised 31 August 2022; accepted 22 September 2022; published 17 October 2022)

We investigate the rotating quark matter in the three-flavor Nambu–Jona-Lasinio (NJL) model. The chiral condensation, spin polarization, and number susceptibility of the light and strange quarks are carefully studied at finite temperatures without or with finite chemical potential in this model. We find that the rotation suppresses the chiral condensation and enhances the first-order quark spin polarization, however for the second-order quark spin polarization and quark number susceptibility the effect is complicated and interesting. When extending to the situation with finite chemical potential, we find the angular velocity also plays a crucial role, at small angular velocity the chemical potential enhances the susceptibility, however in the middle region of angular velocity the effect of the chemical potential is suppressed by the angular velocity and susceptibility can be changed considerably, it can be observed that at very low temperature in the presence of quark chemical potential the quark number susceptibility has two maxima with increasing angular velocity. Furthermore, it is found that at sufficiently large angular velocity the contributions played by the light quark and the strange quark to these phenomena are almost equal. We also discuss the chiral phase transition of rotating quark matter in the three-flavor NJL model. We expect these studies to be used to understand the chiral symmetry breaking and restoration as well as probe the QCD phase transition.

DOI: 10.1103/PhysRevD.106.076007

I. INTRODUCTION

QCD thermodynamics has always been the subject of intense investigations for many years, which motivates various works to try to understand it better. In the past, much attention has been paid to the properties of QCD in the plane of temperature T and quark chemical potential μ. Recently, QCD matter under rotation is of particular interest, since there exist some interesting phenomena in rotating QCD matter, such as the chiral vortical effect or chiral vortical wave [1–4], which is a key ingredient in theories that predict observable effects associated with chiral symmetry restoration and the production of false QCD vacuum states [5]. Many works can be investigated in various rotation-related phenomena, such as noncentral heavy-ion collisions in high energy nuclear physics [6–14], the mesonic condensation of isospin matter with rotation in hadron physics [15], the trapped nonrelativistic bosonic cold atoms in condensed matter physics [16–20], the rapidly spinning neutron stars in astrophysics [21–29]. Quark matter under rotation has been studied in ultrarelativistic heavy-ion off-central collisions performed at the Relativistic Heavy Ion Collider (RHIC) or the Large Hadron Collider (LHC) as well as lattice simulation. It is known that for the region with very low temperature and very large chemical potential there exists uncertainty in lattice QCD due to the "sign problem." Reference [30] has calculated the angular momenta of gluons and quarks in the rotating QCD vacuum, which would be very important for future theoretical research.

One interesting phenomenon is the quark spin polarization in noncentral collisions of heavy ions, where the quark-gluon plasma (QGP) can be generated. The coupling between rotational motion and quantum spin in this plasma can lead to polarization of hadrons along the direction of the system angular momentum. This polarization provides very valuable information about the QGP properties and can be measured experimentally with hyperons via parity-violating weak decays [31–42]. Experimental measurements of the Λ hyperon polarization have been investigated at RHIC and LHC, which would be very helpful in the study of the

*sunfei@ctgu.edu.cn
†huanganping@ucas.ac.cn

hottest, least viscous and most vortical-fluid ever produced both for theoretical physics and experimental physics. Recently, the global spin polarizations of Λ and $\bar{\Lambda}$ have been measured by the STAR collaboration in $\mathrm{Au}+\mathrm{Au}$ collisions over a wide range of beam energies $\sqrt{s_{NN}}=$ 7.7–200 GeV and by ALICE collaboration in $\mathrm{Pb}+\mathrm{Pb}$ collisions at 2.76 TeV and 5.02 TeV [43–45]. On the other hand, theoretical research of spin polarization in the quark matter has been explored [46–53], which plays an important role to explain the origin of the strong magnetic field in the magnetar as well as in changing the dynamical mass and some other phenomena related to the chiral phase transition. It would be very interesting to take into account the influence of the rotating effect on the quark spin polarization, especially, in the case of s quark matter under rotation. The study of quark spin polarization which is linked to vorticity may help us understand the vortical nature of QGP and the chiral dynamics of the system.

Another interesting phenomenon in noncentral collisions of heavy ions is the fluctuations and correlations of conserved charges as quantified by the corresponding susceptibilities, which are sensitive observable quantities in relativistic heavy-ion collisions and are also considered as a useful probe for QGP [54–64]. In this paper, we mainly focus on the baryon number fluctuation which is also simply related to the quark number susceptibility (QNS). QNS serves as a signature for the QGP formation in the ultrarelativistic heavy-ion collision and also plays an important factor to probe the QCD phase transition, as well as the equation of state (EOS) of strongly interacting matter [65–67]. Experimentally, various cumulants of net-kaon multiplicity distributions of $\mathrm{Au}+\mathrm{Au}$ collisions at $\sqrt{s_{NN}}=7.7$–200 GeV have been measured by the STAR experiment [68–70], which are related to the thermodynamic susceptibilities. The study of QNS in lattice QCD has been interesting [71–75]. Although susceptibilities have been studied in the past [76–79], it has not been checked what is the influence of considering the contribution from the strange quark matter [80–91] in the rotation system.

In this paper, encouraged by the successful description of two-flavor QCD under rotation [92] in the Nambu–Jona-Lasinio (NJL) model, which embodies the spontaneous breaking of chiral symmetry via effective interactions between quarks, we further study the three-flavor NJL model in the framework of quarks under rotation. Since there are several flavors and colors of quarks, several pairings are possible, which probably lead to a great variety of interesting phenomena. The questions we are going to address are how the chiral condensate, quark spin polarization, and quark number susceptibility are influenced by the rotation.

Our work is organized as follows. We first discuss the formalism of the three-flavor NJL model in the presence of rotation in Sec. II, by using the mean-field approach and the finite temperature field methods we obtain the grand potential of the fermions with rotation, and the corresponding analytical expressions for the gap equation, spin polarization and susceptibility of the quarks are given. Section III presents numerical results and discussions in detail. Section IV summarizes and concludes the paper. A brief description of fermions under rotation is given in Appendix, which describes the complete set of commuting operators in cylindrical coordinates and derives the eigenstates of these operators.

II. FORMALISM

We start from the three-flavor NJL Lagrangian without rotation [93]:

$$\mathcal{L}=\bar{\psi}(i\partial_\mu\gamma^\mu-m)\psi+G\sum_{a=0}^{8}[(\bar{\psi}\lambda^a\psi)^2+(\bar{\psi}i\gamma^5\lambda^a\psi)^2]+\mathcal{L}_{\mathrm{det}}, \tag{1}$$

here, ψ is the quark field, m is the bare quark mass matrix, $\lambda^a(a=1,\ldots 8)$ are the Gell-Mann matrices in flavor space with $\lambda^0=\sqrt{\frac{2}{3}}\mathbf{1}$ where $\mathbf{1}$ is the unit matrix in the three-flavor space, and $\mathcal{L}_{\mathrm{det}}$ is given by

$$\mathcal{L}_{\mathrm{det}}=-K\{\det[\bar{\psi}(1+\gamma^5)\psi]+\det[\bar{\psi}(1-\gamma^5)\psi]\}, \tag{2}$$

which is known as the six-quark 't Hooft term. Here the determinant is calculated over the flavor degrees of freedom. This term leads to mixing among the different flavors and is also phenomenologically important to get the mass splitting of the η and η' mesons.

In order to derive the grand thermodynamical potential, we use the mean field approximation which means fluctuations are assumed to be small to linearize the Lagrangian. This is done to get a Lagrangian that is quadratic in the quarks fields and which allows the integration of the quarks fields in the generating functional. After a large number of quark interactions be brought to 2-quark interaction [93–98] and neglecting the higher order fluctuations, the Lagrangian reads (note that, for our purposes, only the scalar condensate will contribute, so the pseudoscalar interaction has been dropped [93]):

$$\begin{aligned}\mathcal{L}=&\bar{\psi}(i\partial_\mu\gamma^\mu-M)\psi-2G(\langle\bar{u}u\rangle^2+\langle\bar{d}d\rangle^2+\langle\bar{s}s\rangle^2)\\&+4K\langle\bar{u}u\rangle\langle\bar{d}d\rangle\langle\bar{s}s\rangle,\end{aligned} \tag{3}$$

where we have defined the dynamical quark mass M as follows

$$\begin{aligned}M_{f_i}=&m_{f_i}-4G\langle\bar{\psi}_{fi}\psi_{f_i}\rangle+2K\langle\bar{\psi}_{fj}\psi_{f_j}\rangle\langle\bar{\psi}_{fk}\psi_{f_k}\rangle\\&\times(i\neq j\neq k),\end{aligned} \tag{4}$$

where i, j, k denote the flavor of the quarks and take u, d for two light flavors while s for strange quark.

The condensation of the QCD matter under the presence of rotation in the 2-flavor NJL model has been investigated in Ref. [92], which exhibits interesting behavior for the paring phenomena. In the present work, we will extend to study the properties of the quark matter under rotation in 3-flavor NJL model with finite quark chemical potential. The Lagrangian for spinor with rotation can be written in the following way:

$$\mathcal{L} = \sum \bar{\psi}_f (i\bar{\gamma}^\mu(\partial_\mu + \Gamma_\mu) - m + \gamma^0\mu)\psi_f + G\sum_{a=0}^{8}(\bar{\psi}\lambda^a\psi)^2 + \mathcal{L}_{\rm det}, \tag{5}$$

here $\bar{\gamma}^\mu = e_a{}^\mu\gamma^a$ with $e_a{}^\mu$ the tetrads for spinors, $\Gamma_\mu = \frac{1}{4}\times\frac{1}{2}[\gamma^a,\gamma^b]\Gamma_{ab\mu}$ which is the spinor connection, where $\Gamma_{ab\mu} = \eta_{ac}(e^c{}_\sigma G^\sigma{}_{\mu\nu} e_b{}^\nu - e_b{}^\nu\partial_\mu e^c{}_\nu)$, and $G^\sigma{}_{\mu\nu}$ is the affine connection determined by $g^{\mu\nu}$. Considering the system with an angular velocity along the fixed z-axis, then $\vec{v} = \vec{\omega}\times\vec{x}$ and choosing $e^a{}_\mu = \delta^a{}_\mu + \delta^a{}_i\delta^0{}_\mu v_i$ and $e_a{}^\mu = \delta_a{}^\mu - \delta_a{}^0\delta_i{}^\mu v_i$ (details can be found in Refs. [16,30]), then we can expand the Lagrangian to the first order of angular velocity, finally, the Lagrangian is given by

$$\mathcal{L} = \bar{\psi}[i\gamma^\mu\partial_\mu - m + \gamma^0\mu + (\gamma^0)^{-1}((\vec{\omega}\times\vec{x}) \cdot(-i\vec{\partial}) + \vec{\omega}\cdot\vec{S}_{4\times4})]\psi + G\sum_{a=0}^{8}(\bar{\psi}\lambda^a\psi)^2 + \mathcal{L}_{\rm det}, \tag{6}$$

where we can see as a result of rotation the Dirac operator includes the orbit-rotation coupling term and the spin-rotation coupling term.

The general definition of the partition function can be written as

$$\mathcal{Z} = \int D[\bar{\psi}]D[\psi]e^{iS}, \tag{7}$$

here, S denotes the quark action, which is the integral of the Lagrangian density $\mathcal{L}$.

After using the mean field approximation and carrying out the general approach of the path integral formulation for Grassmann variables, we are now able to exactly integrate out the fermionic fields and obtain

$$\log\mathcal{Z} = -\frac{1}{T}\int d^3x(-2G(\langle\bar{u}u\rangle^2 + \langle\bar{d}d\rangle^2 + \langle\bar{s}s\rangle^2) + 4K\langle\bar{u}u\rangle\langle\bar{d}d\rangle\langle\bar{s}s\rangle) + \sum_f \log\ \det\frac{D_f^{-1}}{T}, \tag{8}$$

here

$$D^{-1} = \gamma^0\left(-i\omega_l + \left(n+\frac{1}{2}\right)\omega + \mu\right) - M - \vec{\gamma}\cdot\vec{p}, \tag{9}$$

which is the inverse of propagator for quarks, and

$$\log\det\frac{\hat{D}^{-1}}{T} = tr\log\frac{\hat{D}^{-1}}{T} = \int d^3x\int\frac{d^3p}{(2\pi)^3}\langle\psi_p(x)|\log\hat{D}^{-1}|\psi_p(x)\rangle. \tag{10}$$

The Dirac fields can be defined in the terms of the wave functions $u(x)$, $v(x)$

$$\psi_p(x) = \sum_{E,n,s,p}(u(x) + v(x)). \tag{11}$$

In order to find solutions of the Dirac equation, we should first choose the complete set of commutating operators that consists of the Hamiltonian of the system $\hat{H}$, the momentum in the z-direction $\hat{p}_z$, the square of transverse momentum $\hat{p}_t^2$, the z-component of the total angular momentum $\hat{J}_z$, and the transverse helicity $\hat{h}_t$. The positive and negative energy solutions of the Dirac field can be determined by calculating these eigenvalue equations of the complete set of commutating operators $\{\hat{H},\hat{p}_z,\hat{p}_t^2,\hat{J}_z,\hat{h}_t\}$, here, for the derivation and detailed expression of the spinor u, v, the reader can analyze the Appendix. By substituting Eq. (11) into Eq. (10) we have:

$$\log\ \det\frac{\hat{D}^{-1}}{T} = \sum_{E,n,s,p} tr\log\frac{D_{u(x)}^{-1}}{T}\int d^3x\int\frac{d^3p}{(2\pi)^3}(\langle u(x)|u(x)\rangle) \tag{12}$$

$$+\sum_{E,n,s,p} tr\log\frac{D_{v(x)}^{-1}}{T}\int d^3x\int\frac{d^3p}{(2\pi)^3}(\langle v(x)|v(x)\rangle), \tag{13}$$

here, the concrete form of the D_u^{-1} that has been considered the rotation and nonzero chemical potential is

$$D^{-1}_{u(x)} = \begin{pmatrix} (-i\omega_l + (n+\frac{1}{2})\omega + \mu) - M & -\vec{\sigma}\cdot\vec{p} \\ \vec{\sigma}\cdot\vec{p} & -(-i\omega_l + (n+\frac{1}{2})\omega + \mu) - M \end{pmatrix}, \tag{14}$$

which corresponds to the positive energy solution, and the concrete form for the D_v^{-1} is

$$D^{-1}_{v(x)} = \begin{pmatrix} (i\omega_l - (n+\frac{1}{2})\omega + \mu) - M & -\vec{\sigma}\cdot\vec{p} \\ \vec{\sigma}\cdot\vec{p} & -(i\omega_l - (n+\frac{1}{2})\omega + \mu) - M \end{pmatrix}, \tag{15}$$

which corresponds to the negative energy solution. Here, in order to study the rotating system at finite density, we have introduced quark chemical potential μ and note that the term $(n+\frac{1}{2})\omega$ in above expressions denotes the rotational polarization energy, which is very useful when we study the polarization in the following sections. By using the general methods in the finite temperature fields [99], we obtain

$$\begin{aligned}\log\ \det\frac{D_u^{-1}}{T} &= \beta\Big(\sqrt{M^2+\mathrm{p}_t^2+\mathrm{p}_z^2} + \Big(n+\frac{1}{2}\Big)\omega\Big) \\ &+ \log(e^{\beta(\sqrt{M^2+\mathrm{p}_t^2+\mathrm{p}_z^2}+((n+\frac{1}{2})\omega-\mu))}+1) \\ &+ \log(e^{\beta(\sqrt{M^2+\mathrm{p}_t^2+\mathrm{p}_z^2}+((n+\frac{1}{2})\omega+\mu))}+1),\end{aligned} \tag{16}$$

and

$$\begin{aligned}\log\ \det\frac{D_v^{-1}}{T} &= \beta\Big(-\sqrt{M^2+\mathrm{p}_t^2+\mathrm{p}_z^2} - \Big(n+\frac{1}{2}\Big)\omega\Big) \\ &+ \log(e^{\beta(-\sqrt{M^2+\mathrm{p}_t^2+\mathrm{p}_z^2}+(-(n+\frac{1}{2})\omega-\mu))}+1) \\ &+ \log(e^{\beta(-\sqrt{M^2+\mathrm{p}_t^2+\mathrm{p}_z^2}+(-(n+\frac{1}{2})\omega+\mu))}+1),\end{aligned} \tag{17}$$

for each flavor, here β is the inverse temperature and the inner products of $\langle u_{n,s}|u_{n,s}\rangle$, $\langle v_{n,s}|v_{n,s}\rangle$ are derived with very simple expressions as follows,

$$\int\frac{d^3p}{(2\pi)^3}\langle u_{n,s}|u_{n,s}\rangle = \frac{1}{2}(J_n(p_tr)^2 + J_{n+1}(p_tr)^2), \tag{18}$$

$$\int\frac{d^3p}{(2\pi)^3}\langle v_{n,s}|v_{n,s}\rangle = \frac{1}{2}(J_n(p_tr)^2 + J_{n+1}(p_tr)^2). \tag{19}$$

Combining the Eqs. (8), (16), (17), (18), and (19) one can now derive the expression of the grand potential for strange quark when the momentum summation turns into the integral

$$\sum_p \to V\int\frac{d^3p}{(2\pi)^3}, \tag{20}$$

and the energy summation performs over Matsubara frequency. Then the thermodynamic grand potential $\Omega = -\frac{T}{V}\log\mathcal{Z}$ has the following expression,

$$\begin{aligned}\Omega = {} & 2G(2\langle\bar{u}u\rangle^2 + \langle\bar{s}s\rangle^2) - 4K\langle\bar{u}u\rangle^2\langle\bar{s}s\rangle - \frac{2N_c}{8\pi^2}\sum_{n=-\infty}^{\infty}\int_0^{\Lambda}\mathrm{p}_t d\mathrm{p}_t\int_{-\sqrt{\Lambda^2-p_t^2}}^{\sqrt{\Lambda^2-p_t^2}}dp_z((J_{n+1}(\mathrm{p}_tr)^2 + J_n(\mathrm{p}_tr)^2) \\ & \times T\Big\{\log\Big(e^{-\frac{-\mu_u+\sqrt{M_u^2+\mathrm{p}_t^2+\mathrm{p}_z^2}-(n+\frac{1}{2})\omega}{T}}+1\Big) + \log\Big(e^{\frac{-\mu_u+\sqrt{M_u^2+\mathrm{p}_t^2+\mathrm{p}_z^2}-(n+\frac{1}{2})\omega}{T}}+1\Big) \\ & + \log\Big(e^{-\frac{\mu_u+\sqrt{M_u^2+\mathrm{p}_t^2+\mathrm{p}_z^2}-(n+\frac{1}{2})\omega}{T}}+1\Big) + \log\Big(e^{\frac{\mu_u+\sqrt{M_u^2+\mathrm{p}_t^2+\mathrm{p}_z^2}-(n+\frac{1}{2})\omega}{T}}+1\Big)\Big\} \\ & - \frac{N_c}{8\pi^2}\sum_{n=-\infty}^{\infty}\int_0^{\Lambda}\mathrm{p}_t d\mathrm{p}_t\int_{-\sqrt{\Lambda^2-p_t^2}}^{\sqrt{\Lambda^2-p_t^2}}dp_z((J_{n+1}(\mathrm{p}_tr)^2 + J_n(\mathrm{p}_tr)^2) \\ & \times T\Big\{\log\Big(e^{-\frac{-\mu_s+\sqrt{M_s^2+\mathrm{p}_t^2+\mathrm{p}_z^2}-(n+\frac{1}{2})\omega}{T}}+1\Big) + \log\Big(e^{\frac{-\mu_s+\sqrt{M_s^2+\mathrm{p}_t^2+\mathrm{p}_z^2}-(n+\frac{1}{2})\omega}{T}}+1\Big) \\ & + \log\Big(e^{-\frac{\mu_s+\sqrt{M_s^2+\mathrm{p}_t^2+\mathrm{p}_z^2}-(n+\frac{1}{2})\omega}{T}}+1\Big) + \log\Big(e^{\frac{\mu_s+\sqrt{M_s^2+\mathrm{p}_t^2+\mathrm{p}_z^2}-(n+\frac{1}{2})\omega}{T}}+1\Big)\Big\}.\end{aligned} \tag{21}$$

Here, the isospin symmetry has been considered for the light quarks, so $m_d = m_u$, $\mu_d = \mu_u$, $N_c = 3$ and Λ is the three-momentum cutoff. μ_u is the chemical potential for the u or d quark as well as μ_s is that for s quark. When the isospin symmetry is satisfied, the dynamical quark masses are simplified to give:

$$M_u = m_u + (2K\langle\bar{s}s\rangle - 4G)\langle\bar{u}u\rangle, \tag{22}$$

$$M_s = m_s - 4G\langle\bar{s}s\rangle + 2K\langle\bar{u}u\rangle^2. \tag{23}$$

We have discussed the grand potential of quarks under rotation in detail in the previous section. In this section, we list our final analytical expressions of the gap equation, quark spin polarization, and quark number susceptibility in the situation with rotation. First, we consider the gap equation which will be required to minimize the grand potential, the values are determined by solving the stationary condition, namely, $\frac{\partial\Omega}{\partial\langle\bar{u}u\rangle} = \frac{\partial\Omega}{\partial\langle\bar{s}s\rangle} = 0$, and the detailed expressions for the stationary condition are listed as follows,

$$\begin{aligned}
&8G\langle\bar{u}u\rangle - 8K\langle\bar{u}u\rangle\langle\bar{s}s\rangle - \frac{N_c}{8\pi^2}\sum_{n=-\infty}^{\infty}\int_0^{\Lambda}\mathrm{p}_t d\mathrm{p}_t\int_{-\sqrt{\Lambda^2-p_t^2}}^{\sqrt{\Lambda^2-p_t^2}} dp_z((J_{n+1}(\mathrm{p}_t r)^2 + J_n(\mathrm{p}_t r)^2)\\
&\times\left\{\frac{4\times 2\times e^{\frac{\mu_u}{T}}\left(e^{\frac{2n\omega+\omega}{T}} - e^{\frac{2\sqrt{M_u^2+p_t^2+p_z^2}}{T}}\right)(2G - K\langle\bar{s}s\rangle)M_u}{\sqrt{M_u^2+p_t^2+p_z^2}\left(e^{\frac{\sqrt{M_u^2+p_t^2+p_z^2}}{T}} + e^{\frac{2n\omega+2\mu_u+\omega}{2T}}\right)\left(e^{\frac{\sqrt{M_u^2+p_t^2+p_z^2}+\mu_u}{T}} + e^{\frac{(n+\frac{1}{2})\omega}{T}}\right)}\right.\\
&\left.-\frac{8Ke^{\frac{\mu_s}{T}}\left(e^{\frac{2n\omega+\omega}{T}} - e^{\frac{2\sqrt{M_s^2+p_t^2+p_z^2}}{T}}\right)\langle\bar{u}u\rangle M_s}{\sqrt{M_s^2+p_t^2+p_z^2}\left(e^{\frac{\sqrt{M_s^2+p_t^2+p_z^2}}{T}} + e^{\frac{2n\omega+2\mu_s+\omega}{2T}}\right)\left(e^{\frac{\sqrt{M_s^2+p_t^2+p_z^2}+\mu_s}{T}} + e^{\frac{(n+\frac{1}{2})\omega}{T}}\right)}\right\} = 0,
\end{aligned} \tag{24}$$

$$\begin{aligned}
&4G\langle\bar{s}s\rangle - 4K\langle\bar{u}u\rangle^2 - \frac{N_c}{8\pi^2}\sum_{n=-\infty}^{\infty}\int_0^{\Lambda}\mathrm{p}_t d\mathrm{p}_t\int_{-\sqrt{\Lambda^2-p_t^2}}^{\sqrt{\Lambda^2-p_t^2}} dp_z((J_{n+1}(\mathrm{p}_t r)^2 + J_n(\mathrm{p}_t r)^2)\\
&\times\left\{-\frac{4\times 2\times Ke^{\frac{\mu_u}{T}}\left(e^{\frac{2n\omega+\omega}{T}} - e^{\frac{2\sqrt{M_u^2+p_t^2+p_z^2}}{T}}\right)\langle\bar{u}u\rangle M_u}{\sqrt{M_u^2+p_t^2+p_z^2}\left(e^{\frac{\sqrt{M_u^2+p_t^2+p_z^2}}{T}} + e^{\frac{2n\omega+2\mu_u+\omega}{2T}}\right)\left(e^{\frac{\sqrt{M_u^2+p_t^2+p_z^2}+\mu_u}{T}} + e^{\frac{(n+\frac{1}{2})\omega}{T}}\right)}\right.\\
&\left.\times\frac{8Ge^{\frac{\mu_s}{T}}\left(e^{\frac{2n\omega+\omega}{T}} - e^{\frac{2\sqrt{M_s^2+p_t^2+p_z^2}}{T}}\right)M_s}{\sqrt{M_s^2+p_t^2+p_z^2}\left(e^{\frac{\sqrt{M_s^2+p_t^2+p_z^2}}{T}} + e^{\frac{2n\omega+2\mu_s+\omega}{2T}}\right)\left(e^{\frac{\sqrt{M_s^2+p_t^2+p_z^2}+\mu_s}{T}} + e^{\frac{(n+\frac{1}{2})\omega}{T}}\right)}\right\} = 0.
\end{aligned} \tag{25}$$

Here we are going to study the quark spin polarization which can be defined as taking the partial derivative of minus grand potential with respect to angular velocity, and we introduce the following quark spin polarization as in Ref. [100]

$$\mathcal{P}_1 = \frac{\partial(\frac{-\Omega}{T^4})}{\partial(\frac{\omega}{T})}, \tag{26}$$

$$\mathcal{P}_2 = \frac{\partial^2(\frac{-\Omega}{T^4})}{\partial(\frac{\omega}{T})^2}, \tag{27}$$

such definition ensures dimensionless polarization, then we list the detailed expression of the first-order polarization and second-order polarization as follows,

$$\begin{aligned}
\mathcal{P}_1 = &\frac{N_c}{8\pi^2T^3}\sum_{n=-\infty}^{\infty}\int_0^{\Lambda}\mathrm{p}_t d\mathrm{p}_t\int_{-\sqrt{\Lambda^2-p_t^2}}^{\sqrt{\Lambda^2-p_t^2}} dp_z((J_{n+1}(\mathrm{p}_t r)^2 + J_n(\mathrm{p}_t r)^2)(2n+1)\\
&\times\left\{\frac{2\sinh\left(\frac{-2\sqrt{M_u^2+\mathrm{p}_t^2+\mathrm{p}_z^2}+2n\omega+\omega}{2T}\right)}{\left(\cosh\left(\frac{-2\sqrt{M_u^2+\mathrm{p}_t^2+\mathrm{p}_z^2}+2n\omega+\omega}{2T}\right) + \cosh(\frac{\mu_u}{T})\right)} + \frac{\sinh\left(\frac{-2\sqrt{M_s^2+\mathrm{p}_t^2+\mathrm{p}_z^2}+2n\omega+\omega}{2T}\right)}{\left(\cosh\left(\frac{-2\sqrt{M_s^2+\mathrm{p}_t^2+\mathrm{p}_z^2}+2n\omega+\omega}{2T}\right) + \cosh(\frac{\mu_s}{T})\right)}\right\},
\end{aligned} \tag{28}$$

$$\mathcal{P}_2 = \frac{N_c}{64\pi^2 T^3}\sum_{n=-\infty}^{\infty}\int_0^{\Lambda} \mathrm{p}_t d\mathrm{p}_t \int_{-\sqrt{\Lambda^2-p_t^2}}^{\sqrt{\Lambda^2-p_t^2}} dp_z((J_{n+1}(\mathrm{p}_t r)^2 + J_n(\mathrm{p}_t r)^2)(2n+1)^2$$
$$\times\left\{2\left(\mathrm{sec\,h}^2\left(\frac{2\mu_u - 2\sqrt{M_u^2+\mathrm{pt}^2+\mathrm{pz}^2}+2n\omega+\omega}{4T}\right)+\mathrm{sec\,h}^2\left(\frac{-2\mu_u - 2\sqrt{M_u^2+\mathrm{pt}^2+\mathrm{pz}^2}+2n\omega+\omega}{4T}\right)\right)\right.$$
$$\left.+\left(\mathrm{sec\,h}^2\left(\frac{2\mu_s - 2\sqrt{M_s^2+\mathrm{pt}^2+\mathrm{pz}^2}+2n\omega+\omega}{4T}\right)+\mathrm{sec\,h}^2\left(\frac{-2\mu_s - 2\sqrt{M_s^2+\mathrm{pt}^2+\mathrm{pz}^2}+2n\omega+\omega}{4T}\right)\right)\right\}. \quad (29)$$

Next, we will investigate how much the rotation affects the baryon number fluctuations, these fluctuations can be quantified by the susceptibilities and the QNS is defined through the Taylor expansion coefficients of the pressure over the chemical potential [101–107]:

$$\chi_n = \frac{\partial^n(\frac{P}{T^4})}{\partial(\frac{\mu}{T})^n}, \quad (30)$$

here, we focus on the second order derivative of pressure with respect to μ, due to symmetry, all the odd susceptibilities vanish when $\mu \to 0$ (note, in the context of lattice calculations the susceptibilities are defined as dimensionless quantities). Using the relation of pressure $P = -\Omega$, the actual calculation of the susceptibilities is straightforward and the detailed result is

$$\chi_2^f = \frac{N_c}{16\pi^2 T^3}\sum_{n=-\infty}^{\infty}\int_0^{\Lambda} \mathrm{p}_t d\mathrm{p}_t \int_{-\sqrt{\Lambda^2-p_t^2}}^{\sqrt{\Lambda^2-p_t^2}} dp_z((J_{n+1}(\mathrm{p}_t r)^2 + J_n(\mathrm{p}_t r)^2)$$
$$\times\left(\mathrm{sec\,h}^2\left(\frac{2\mu_f - 2\sqrt{M_f^2+\mathrm{pt}^2+\mathrm{pz}^2}+2n\omega+\omega}{4T}\right)+\mathrm{sec\,h}^2\left(\frac{-2\mu_f - 2\sqrt{M_f^2+\mathrm{pt}^2+\mathrm{pz}^2}+2n\omega+\omega}{4T}\right)\right), \quad (31)$$

here $f = u, d, s$. With the analytical expressions given above, we show our numerical results in the next section.

III. NUMERICAL RESULTS AND DISCUSSIONS

In this section, we will present our numerical results for the gap equation, quark spin polarization, and quark number susceptibility. In our previous analytic expressions, the z-angular-momentum quantum number $n = 0, \pm 1, \pm 2\ldots$. In principle we should sum all the values of n, fortunately, these expressions converge so fast that it is enough for us to sum n from -5 to 5. It should be noted that in order to maintain the causality of a rigidly rotating system, we should make sure that the local velocity is smaller than the light velocity, namely, the condition $\omega r < 1$ should be considered in all the calculations, and for simplicity, we take the same value of r as in Ref. [92]. Since any uniformly rotating system should be spatially bounded, it has been expected that the presence of boundaries can modify the properties of the rotating system [108–112], indeed, this is only true when the angular velocity ω is much smaller than the inverse of the system's size [113]. Furthermore, our discussion is mainly devoted to the bulk properties of the rotating system, so in our analytic derivation, we ignore the finite volume boundary effect and leave it to our further study. In our calculations, for simplicity, we have let the chemical potential $\mu_{u/d} = \mu_s = \mu$, and the input parameters in the NJL are the coupling constants G, K, the quark masses $m_{u/d}$, m_s and the three-momentum cutoff Λ. Then, in this context we use the second case in Table 1 of Ref. [114], that $m_u = m_d = 0.005$ GeV, $m_s = 0.1283$ GeV, $G = 3.672$ GeV^{-2}, $K = 59.628$ GeV^{-5}, $\Lambda = 0.6816$ GeV, which have been estimated by the fitting in light of the following observations: $m_\pi = 138$ MeV, $f_\pi = 92$ MeV, $m_K = 495$ MeV and $m_{\eta'} = 958$ MeV.

A. The mean field mass gap at zero chemical potential $\mu = 0$ under rotation

Let us first discuss the results at zero chemical potential. We investigate the chiral condensation in the rotating matter under the three-flavor NJL model, especially we consider the contribution from s quark. It is equivalent to studying the gap equations since the gap equations correspond to the coupling of the current quark masses with the associated chiral condensates, first, in the plot of Fig. 1, we show the differences in squared gap masses between the case at nonzero angular velocity and that at zero angular velocity, $M^2(\omega) - M^2(\omega = 0)$ with zero temperature and zero chemical potential for the up quark and strange quark, respectively. We found that the squared gap mass differences of all quarks decrease with increasing angular velocity, and at large angular velocity, there is a sudden drop down for the squared gap mass differences. It obvious that the squared gap mass difference of lighter quark is

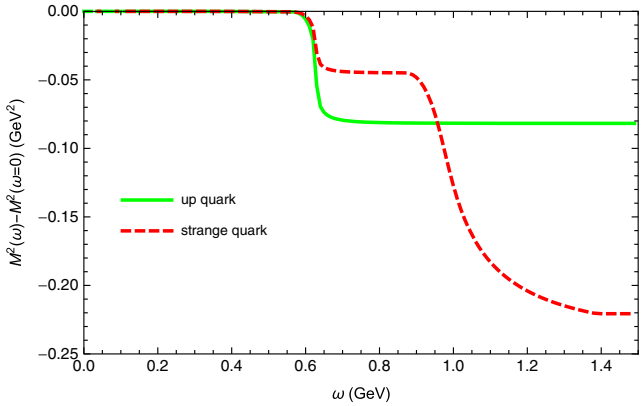

FIG. 1. Differences of squared gap masses between the case at $\omega \neq 0$ and $\omega = 0$ with both $\mu = 0$ and $T = 0$ for up quark and strange quark as a function of ω.

more affected by the angular velocity, which decreases faster while that of the strange quark decreases slower with angular velocity, this can be interpreted as that the quark with a large current mass is less affected by the rotation.

Then we plot the gap equation as a function of ω with different values of T in Fig. 2 respectively for u and s quark. As one can see, both u quark and s quark gap equations show that the rotation has a suppression effect on the chiral condensation. It is clearly seen that at all temperatures the gap equations of both u and s decrease with increasing ω and at very low temperatures the chiral condensate experiences a very sharp transition when ω exceeds a certain value. It should be noted here, that although there is a very fast drop from a high value for the quark effective mass to a small value, however, the phase transition here is just a rapid cross-over. It is very interesting when comparing the different flavor situations, in the left panel of Fig. 2 shows that M_u experiences a very fast transition around $\omega = 0.6$ GeV at $T = 0.01$ GeV, in the right panel of Fig. 2 we observe that M_s also experiences a fast change around $\omega = 0.6$ GeV but changes not so much their mass compared to the light quark situation, due to the coupling between the different flavors. In addition, we also found that for the strange quark there is a fast drop from a high value for the quark effective mass to a small value around $\omega = 1.0$ GeV. From the figure, we can see the role of the ω, as well as T are very important parameters for transition. For high temperatures the chiral condensate vanishes with the increasing ω via a smooth cross-over, and the temperature effect becomes weaker with increasing the value of ω. As ω further increases the gap equations for both decrease more slowly, and both approach their naked masses. This can be interpreted as a hint that the chiral transitions for the s, u do not occur at the same angular velocity with the same temperature. It is found that the chiral condensation of u quark has produced results almost in agreement with those suggested in literature [4], but with a slight difference due to the adopted parameters in Ref. [96].

We now turn to a more realistic physical environment, in Fig. 3 we plot the gap equation as a function of T with fixed angular velocity ω and radius r for u and s quark, respectively. In order to enable a more realistic comparison to experimental data in the future, here without losing generality, we assume that $\omega = 0.01$, 0.1 GeV and $r = 1$, 1.6 fm. From the figure, we can see clearly that there exist some interesting behaviors in the range of $T = 0.1$–0.4 GeV. The left-hand side of Fig. 3 shows that the u quark gap mass decreases with increasing temperature, and the mass gap M_u falls sharply in the range of $T = 0.15$–0.2 GeV, however, it is a smooth behavior which means that at low T, small ω and large radius the quark condensate experiences a fast cross-over transition. Therefore, in this region ($T = 0.15$–0.2 GeV), there occurs not a true phase transition with corresponding critical temperature, but rather a pseudo-phase transition (cross-over). The right-hand side of Fig. 3 shows that for the chosen parameters the s quark gap mass decreases with increasing temperature via a cross-over transition and the chiral condensate gradually vanishes with increasing temperature. From Fig. 3 one can also see clearly that, for a fixed value of r the effect of rotation suppresses the effective quark mass and for a fixed value of small ω

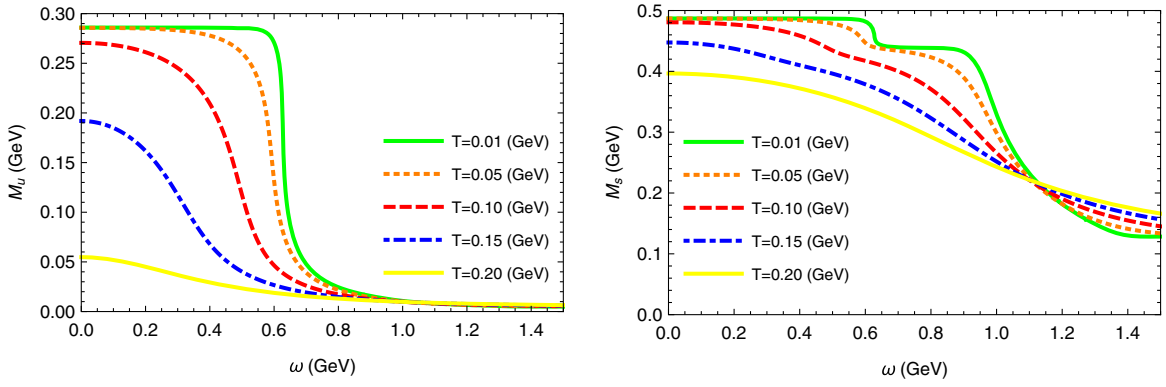

FIG. 2. The mean field mass gap M_u and M_s as a function of ω for several values of T with $\mu = 0$.

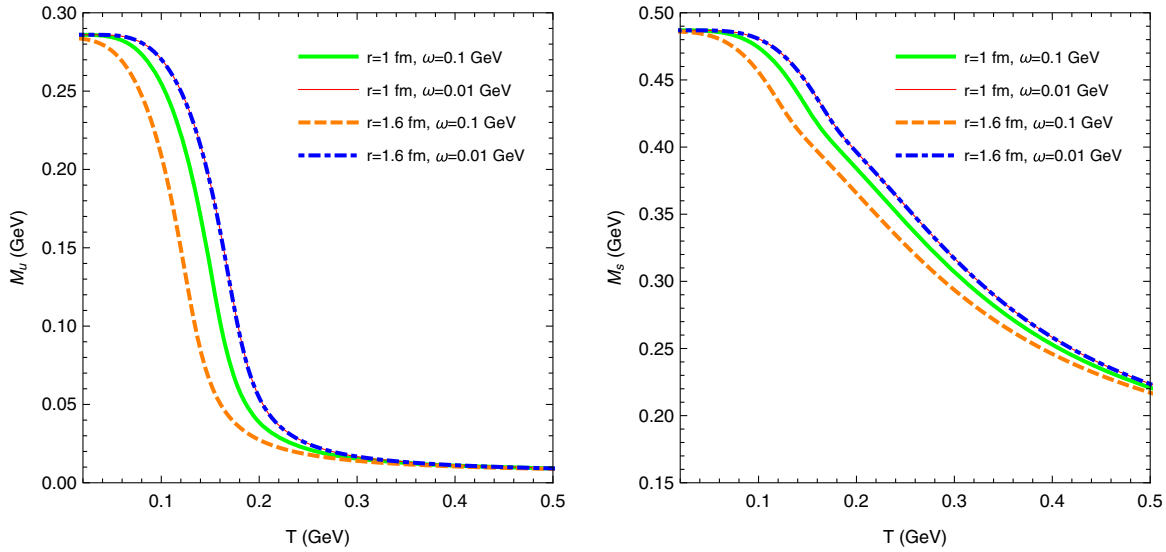

FIG. 3. (Color online) The mean field mass gap M_u and M_s as a function of T for several values of r and ω with $\mu = 0$.

we can observe that the effective quark mass becomes smaller at a larger radius. Here we just want to capture the essential physics of QCD matter under rotation, indeed, in a realistic physical environment, it requires a more detailed investigation.

B. Spin polarization, quark number susceptibility at $\mu = 0$

The logarithmic plot of first-order spin polarizations of the rotating system as a function of ω for several fixed values of temperature with zero chemical potential are shown in Fig. 4. It is very clear that the angular velocity has a strong influence on the quark first-order spin polarization as well as the temperature. From the figure, it is observed that the rotation system may induce a large polarization. At all temperatures, the quark spin polarization increases with increasing angular velocity for all quarks. At low temperatures, the quark first-order spin polarization increases very rapidly in a certain angular velocity window and then increases very slowly, while at high temperatures the quark first-order spin polarization increases almost linearly. At very low temperatures an interesting phenomenon of the jump of the quark first-order spin polarization can be observed around $\omega \sim 0.6$ GeV for the rotating system in the figure. This jump of the first-order spin polarization is a hint for the rapid phase transition to occur, and this distinguishing feature of the spin polarization may provide valuable insights for investigating the rapid phase transition in experiments.

In order to have a better understanding of the spin polarization of quark with rotation, we plot the second-order spin polarizations of the rotating system as a function of ω for several temperatures with the zero chemical potential in Fig. 5. In the case of very low temperatures, the second-order spin polarization begins to grow significantly only after a certain value of the angular velocity, and

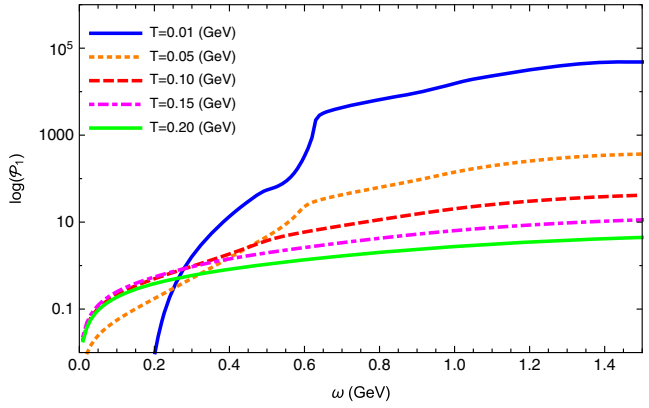

FIG. 4. The logarithmic plot of first-order spin polarizations of the rotating system according to ω for several fixed values of temperature T with $\mu = 0$.

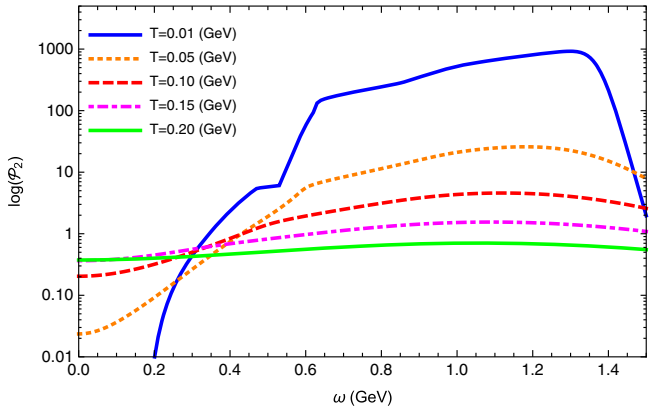

FIG. 5. The logarithmic plot of second-order spin polarizations of the rotating system according to ω for several fixed values of temperature T with $\mu = 0$.

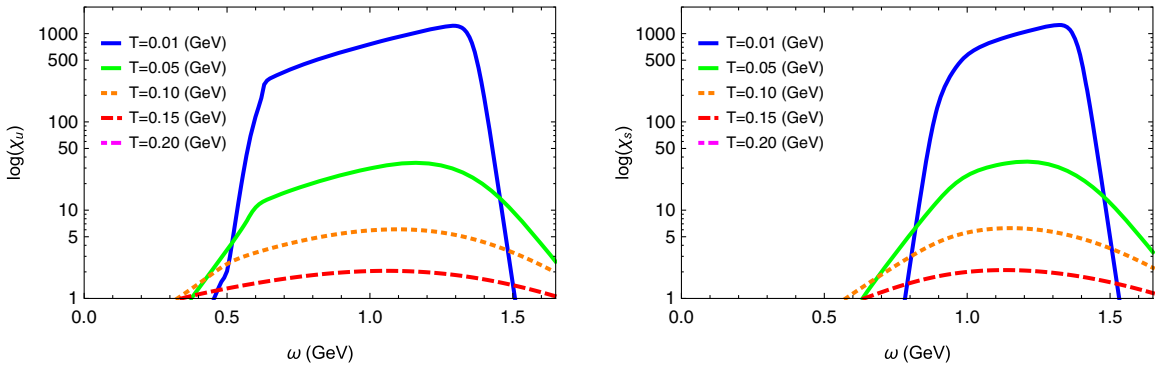

FIG. 6. Susceptibilities of u and s quark as a function of ω for several values of T with $\mu = 0$ in a logarithmic plot.

it continues to increase with increasing angular velocity, until it reaches the highest value, at a point where, if the angular velocity is increased even further the second-order spin polarization becomes weaker. The dominant reason for these tendencies comes from that the rotation under finite temperature leads to the restoration of spontaneously broken chiral symmetry.

On the other hand, in order to understand the properties of the quark matter under rotation better, it is helpful to study the behavior of baryon number susceptibility. We now turn to study the QNS and take into account the influence of angular velocity on QNS. First, we consider the case of zero chemical potential, in Fig. 6 we plot the susceptibilities of u and s quark as a function of angular velocity for several fixed values of temperatures with zero chemical potential in a logarithmic plot. As evident in Fig. 6, the u or s quark number susceptibility increases as the ω increases, until it reaches the highest point. After this point, however, an increase in ω causes a decrease in the quark number susceptibility. It also can be seen from the figure that the temperature and the angular velocity play an important role in the susceptibility, at low temperature chiral symmetry is broken spontaneously, however with the increasing of the angular velocity the chiral symmetry is restored, so we can see at low temperature and low angular velocity the susceptibility is very small and at low temperature and large angular velocity the susceptibility almost disappears. However, if the temperature is high the susceptibility always occurs and the angular velocity plays a small effect on the rotating matter.

Next, we turn to a discussion of the different features of susceptibilities of the light and strange quarks under rotation. When angular velocity is small, we find that it is easier for the susceptibility of u quark compared to s quark to have a significant rising trend. For instance, at $T = 0.01$ GeV, we observe only a very small dependence of susceptibility on angular velocity, as long as $\omega \leq 0.45$ GeV for u quark, while as long as $\omega \leq 0.8$ GeV for s quark.

The susceptibility exhibits a peak as we increase the angular velocity, and at low temperatures, there exists a narrow region where the susceptibility can rapidly change with ω. For the strange quark, you might have a less broad peak, for instance, at temperature $T = 0.01$ GeV, the width of this region is around (0.6–1.4) GeV for χ_u, while the region is around (0.9–1.4) GeV for χ_s. The position of its maximum depends sensitively on temperature. Here, the presence of a peak structure in these observable can be interpreted as a signal of growing fluctuations in the baryon density. At low temperatures, the sharper peak corresponds to a smaller value of temperature. As we increase temperature, we observe a significant decrease in the maximum of the peak, and the location of the maximum moves toward smaller values of angular velocity. It is clear from the figure that at all values of the temperature, the behaviors of the u quark and s quark number susceptibility are very similar with increasing the angular velocity, and the peaks of the susceptibilities appear at almost the same angular velocity. When the angular velocity is large the role played by the mass of different quarks becomes weaker, and finally, can almost be ignored, accordingly, the contribution from the angular velocity becomes dominant to the quark number susceptibilities.

C. Spin polarization, quark number susceptibility at $T = 0.01$ GeV and $\mu \neq 0$

Let us now discuss the behavior of the mean field mass gap of the quark at very low temperature with nonzero chemical potential, in Fig. 7 we plot M_u and M_s as a function of ω for a variety of values of μ at $T = 0.01$ GeV, respectively. Compared with the Fig. 2, it is clear that a nonzero value of the chemical potential affects the phase transition, at $T = 0.01$ GeV, there does not exist a sudden drop for the mean field mass gap when μ is large both for u and s quark, which indicating there exists a suppression effect for the chemical potential on the phase transition. At large chemical potential, the chiral condensate vanishes with increasing ω via a smooth cross-over. From the figure we can also see that there is different behavior between u and s quark, the u quark is more affected by the presence of the chemical potential and angular velocity than s quark

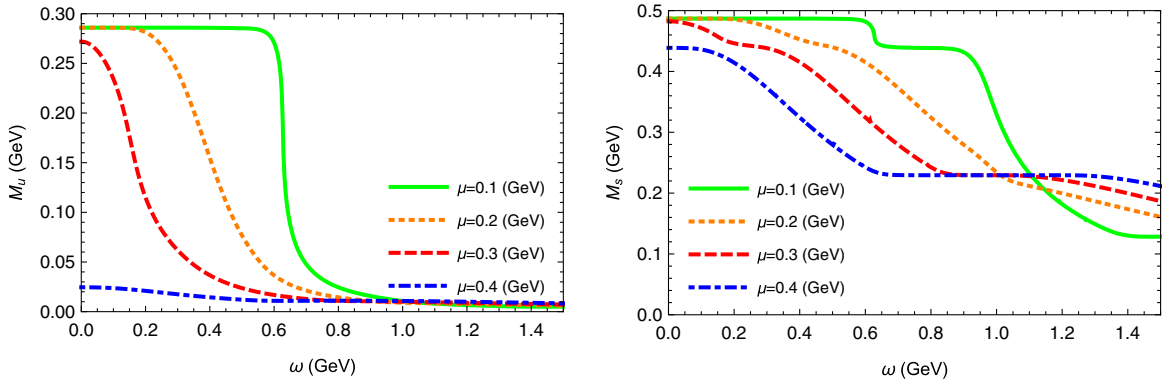

FIG. 7. The mean field mass gap of u and s quark as a function of ω for several fixed values of μ at $T = 0.01$ GeV.

because the s quark has a substantial mass even after the chiral phase transition.

In Fig. 8, the plots of the first-order spin polarization of the rotating system as a function of angular velocity at $T = 0.01$ GeV are presented for nonzero chemical potential $\mu = 0.1, 0.2, 0.3, 0.4$ GeV, respectively. As it is evident from the figure, the first-order spin polarizations of the rotating system increase with increasing angular velocity. It can be seen that the first-order spin polarizations are affected obviously by the nonzero quark chemical potential. With increasing angular velocity, the first-order spin polarization of the system will first have a clear increasing trend at larger quark chemical potential, for example, the first-order spin polarizations of the rotating system start to increase evidently around $\omega = 0.2$ GeV and $\omega = 0.4$ GeV for $\mu = 0.2$ GeV and $\mu = 0.1$ GeV, respectively. Figure 8 also demonstrates that at very large quark chemical potential, the first-order spin polarization of the system first quickly reaches a certain value then is only relatively slowly varying with angular velocity, this can be understood by noting that at a large value of quark chemical potential the chiral symmetry is restored quickly.

Figure 9 displays the results of the second-order polarization of the system as a function of ω for several fixed nonzero values of chemical potential at $T = 0.01$ GeV. In particular, a nonmonotonic is identified, with the second-order polarization to first increase, reach a maximum, and then decrease sharply. This behavior is the combined effect of the suppression in both the angular velocity itself and the chemical potential at very low temperature.

Next, we will analyze the patterns of second-order susceptibility of quark with rotation at nonzero chemical potential. Let us first consider the effect of angular velocity ω on second-order susceptibility of the quarks at very low temperature. We plot the second-order susceptibilities of u and s quark as a function of ω for several fixed nonzero values of chemical potential at $T = 0.01$ GeV in Fig. 10, respectively. From the figure we find the susceptibilities have similar behavior with respect to the angular velocity. We can see if one considers the case of nonzero chemical potential, the behavior of QNS changes considerably and is quite dependent on the angular velocity. As shown in the figure one can see the dependence of QNS on angular velocity is complicated that the QNS increases with the

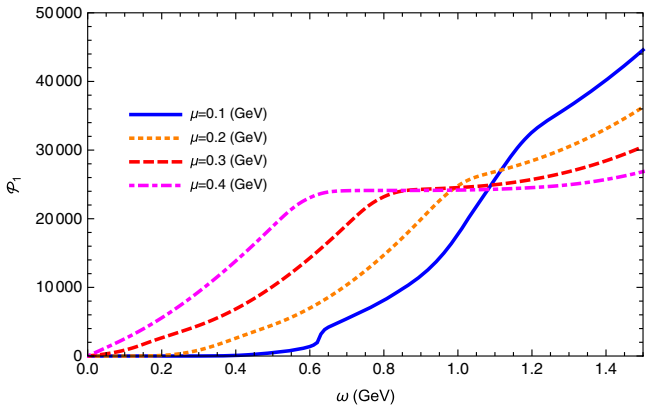

FIG. 8. First-order spin polarizations of the rotating system as a function of ω for several fixed nonzero values of μ at $T = 0.01$ GeV.

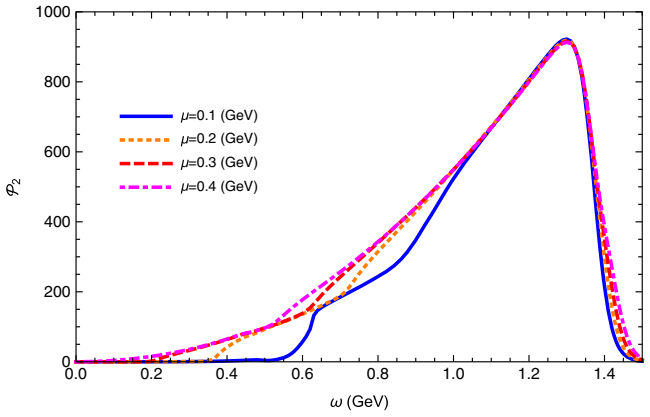

FIG. 9. Second-order spin polarizations of the rotating system as a function of ω for several fixed nonzero values of μ at $T = 0.01$ GeV.

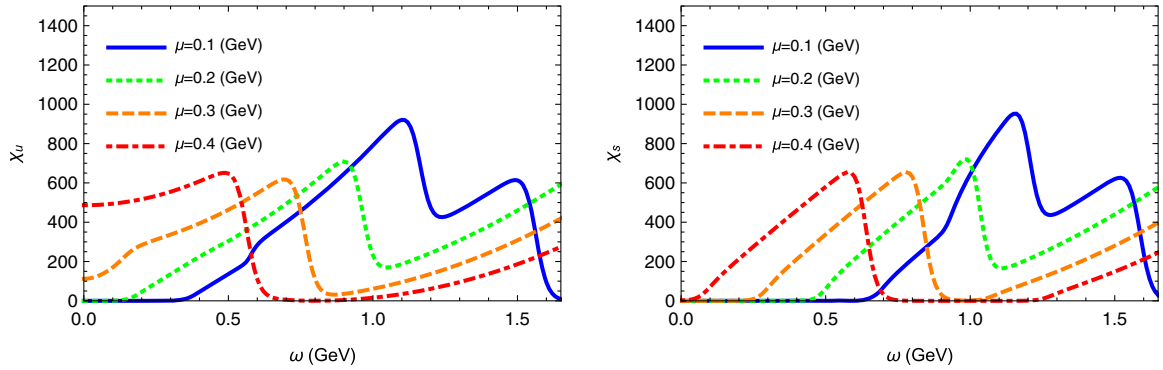

FIG. 10. Susceptibilities of u and s quark as a function of ω for several fixed nonzero values of μ at $T = 0.01$ GeV.

increasing ω when ω is smaller than a certain value while the QNS decreases with the increasing ω when ω exceeds another certain value, such nonmonotonic behavior of the susceptibilities may suggest that more attention should be given to the studies of quark matter under rotation.

There are some interesting changes compared with the situation of zero chemical potential, at $T = 0.01$ GeV the curves of susceptibility of the quark have two peaks, which are very different compared with that in Fig. 6, the curves of QNS have such behavior because the gap mass with nonzero chemical potential is different from that the case with zero chemical potential and for any angular velocity which should satisfy the gap equation, whose constraint will have an effect on the susceptibility. In addition, a plausible explanation for this phenomenon is that the rotational velocity serves as an effective chemical potential and exhibits a nontrivial behavior such that the competition between the chemical potential and angular velocity renders the quark number susceptibility to reach its maximum in such manner.

D. Spin polarization, quark number susceptibility at $T = 0.2$ GeV and $\mu \neq 0$

We now discuss the rotational effect on the quark spin polarization, quark number susceptibility at nonzero chemical potential, and high temperature. Figure 11 shows the mean field mass gap M_u and M_s versus ω with several fixed values of μ at $T = 0.2$ GeV, obviously from the figure we can see there is a generally rotational suppression effect on the chiral condensate for the system at high temperature with nonzero chemical potential. In order to have better understanding in Fig. 12 we plot $M_u(\omega)/M_u(\omega = 0)$ and $M_s(\omega)/M_s(\omega = 0)$ as a function of ω with several nonzero chemical potentials at $T = 0.2$ GeV, respectively. We can see the influence of the angular velocity on the light quark and strange quark is different. The figure shows that M_u is much affected due to the small size of the up quark current mass and whose chiral symmetry can be easily restored compared to that of s quark.

In Fig. 13, we plot the first-order spin polarization of the system as a function of ω for several fixed values of μ with $T = 0.2$ GeV. From Fig. 13 we find that at this temperature the first-order quark spin polarization of the system always occurs with increasing the angular velocity for all the nonzero chemical potential, at large chemical potential ($\mu = 0.4$ GeV), the first-order spin polarization of the system increases almost linearly with increasing the angular velocity. We now consider the effects of angular velocity ω on second-order spin polarization of the system at $T = 0.2$ GeV with chemical potential $\mu = 0.1$, 0.2, 0.3,

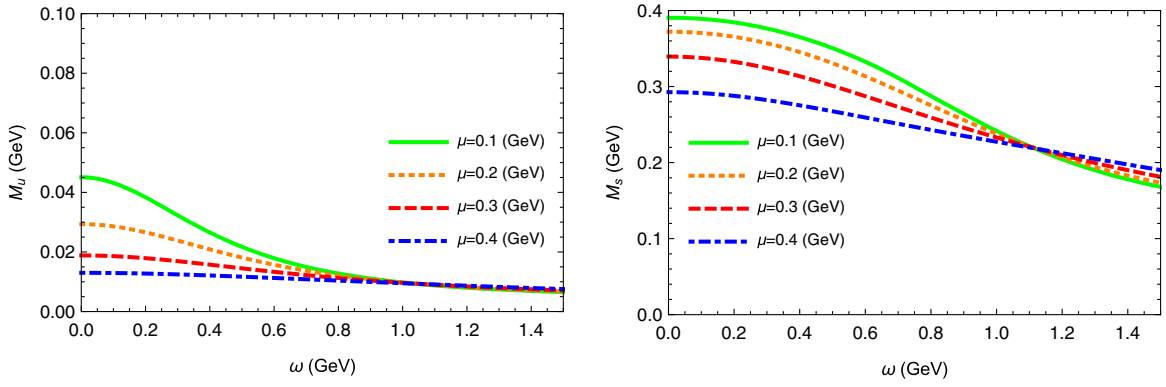

FIG. 11. The mean field mass gap M_u and M_s as a function of ω for several fixed values of μ at $T = 0.2$ GeV.

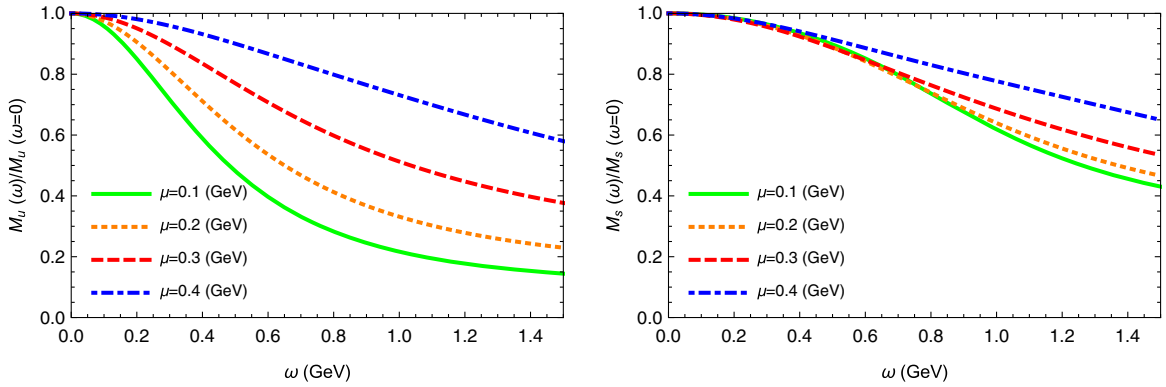

FIG. 12. $M_u(\omega)/M_u(\omega=0)$ and $M_s(\omega)/M_s(\omega=0)$ as a function of ω with several nonzero chemical potentials at $T=0.2$ GeV.

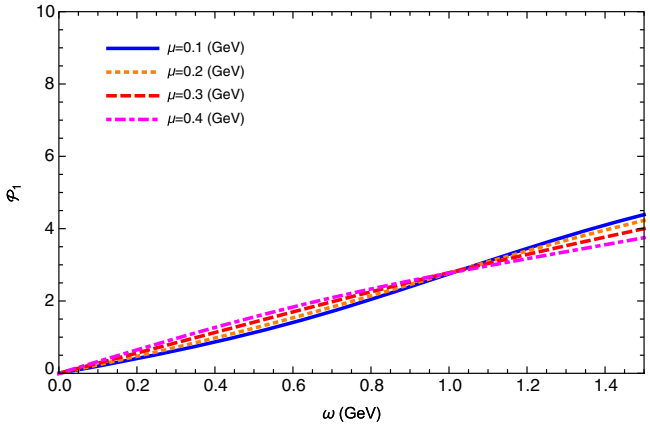

FIG. 13. First-order spin polarizations of the rotating system as a function of ω for several fixed values of μ at $T=0.2$ GeV.

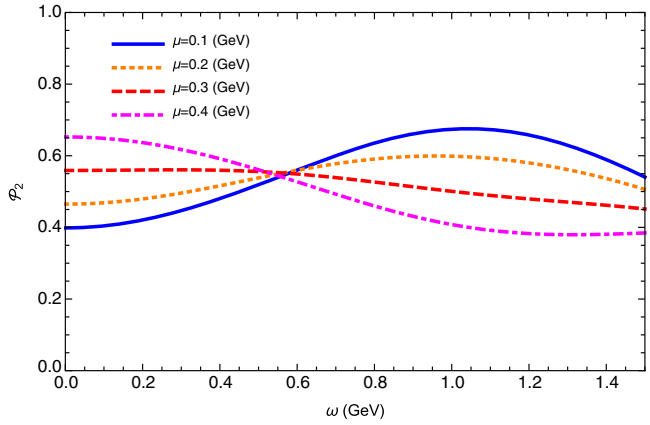

FIG. 14. Second-order spin polarizations of the rotating system as a function of ω for several fixed nonzero values of μ at $T=0.2$ GeV.

0.4 GeV, respectively. From Fig. 14 one immediately makes the following observations, in the case of high temperature the variation of second-order spin polarization of the system with angular velocity is complicated, we find that at small chemical potential the second-order spin polarization of the system has a peak structure with the increase of angular velocity when $\omega < 1.0$ GeV, at small chemical potential ($\mu = 0.1$ GeV) the second-order spin polarization of the system increases with increase in angular velocity, while at large chemical potential ($\mu = 0.4$ GeV) that decreases with increase in angular velocity.

Next, we would like to consider the effects of angular velocity ω on second-order susceptibility of the quarks at high temperature with several fixed nonzero values of chemical potential, and the numerical results are shown in Fig. 15. It can be found that at such high temperatures the second-order susceptibility of the quarks can always occur, although the maximum value of susceptibility is very small compared to the situation in Fig. 10, which means that the contribution of angular velocity to the susceptibility is suppressed by high temperature. From Fig. 15 one could infer the dependence of the second-order susceptibility of the quarks on the quark current mass when $\omega < 0.5$ GeV, the values of the susceptibility of the strange quark is smaller compared to that of light quarks for the same quark chemical potential. However, with the increase of ω, the behavior of both quarks is very similar which means that at high temperature and large chemical potential, the large angular velocity takes a significant role in the behavior of quarks under rotation. From Fig. 15, we can see that in the case of high temperature and large chemical potential, the behavior of both quarks is very similar with the increase of ω, although the strange quark still has an effective mass much larger than its bare mass. From Fig. 15 one could also infer the dependence of susceptibility on the chemical potential at high temperature, at small ω, the susceptibility increases with the increasing μ, at large ω, the susceptibility decreases with the increasing μ.

E. The chiral phase transition of quark matter under rotation

Let us move on to the topic of the QCD phase diagram. The investigation of the phase diagram of QCD has been an active subject for many years. There has been some progress

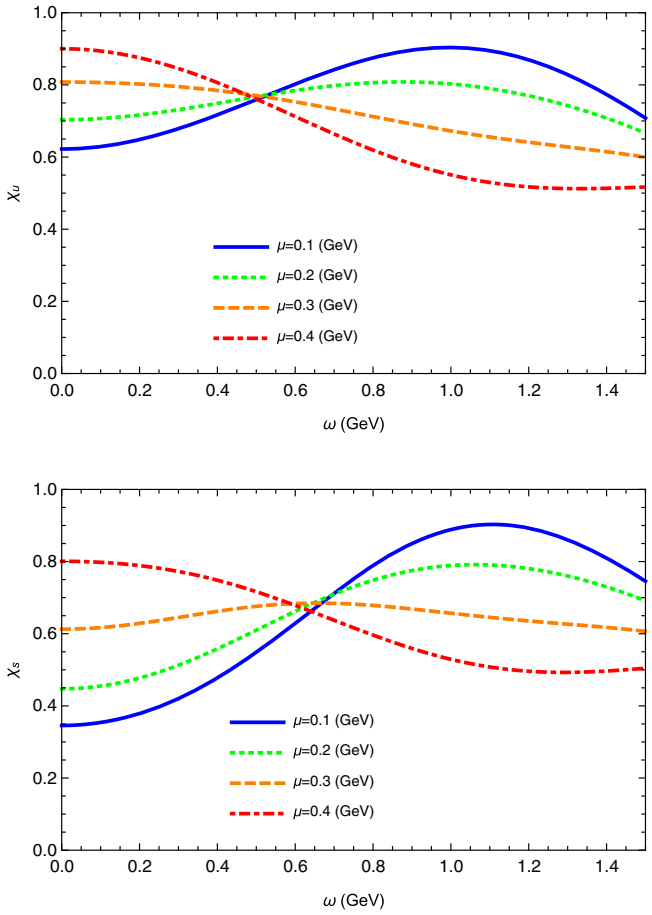

FIG. 15. Second-order susceptibilities of u and s quark as a function of ω for several fixed nonzero values of μ at $T = 0.2$ GeV.

in the study of the QCD phase diagram with lattice QCD (LQCD) simulations [115,116], however, at large chemical potential the predictions made by the LQCD are not very reliable due to the sign problem of lattice gauge theory [117]. So, in order to investigate the QCD phase diagram many effective models have been proposed such as Nambu–Jona-Lasinio (NJL) models, quark-meson (QM) models, holographic QCD models, functional renormalization group (fRG), Dyson Schwinger equations (DSE) as well as some extending modes of these [93,96,118–138]. It is believed that the addition of external influences or new parameter ranges yields an increasing number of interesting results to the phase diagram [139].

Investigating the QCD matter under rotation is a fascinating topic, apart from the chiral condensation, spin polarization, and number susceptibility of quark, it is also of significant interest to explore the effects of rotation on the phase transitions. We now first explore the phase diagram in the T-ω plane, it is obvious that from the Fig. 2 at all temperatures the gap equations of both u and s decrease with increasing ω and at very low temperature the chiral condensate experiences a very fast transition when ω exceeds a certain value. It should be noted here that although there is a very fast drop from a high value for the quark effective mass to a small value, however, the transition here is just a rapid cross-over (in the case of first-order phase transition, the thermodynamical potential should have a region where it is multievaluated for the same value of omega, however, in our parameter space we cannot find such region). This is very different when compared to the quark matter under rotation in the 2-flavor NJL model, in Ref. [92] the authors claim that in the case of chiral condensation, a new phase diagram in the T-ω parameter space is found, with a nontrivial critical point. However, in the 3-flavor NJL model with rotation, we can only find that there exists a rapid cross-over for the chiral condensation. This is maybe be caused by the presence of the heavy strange quark as well as the 't Hooft interaction which will have an effect on the phase transition of the system under rotation.

When the cross-over is sufficiently rapid that the definition of a transition temperature makes sense. This can be defined as the maximum of the chiral susceptibility, which is proportional to the slope of the quark condensate [93]. It is no doubt that there are many other discussions that need to be done for the phase transition in the rotation system, here is just a beginning and this particular topic will be discussed in detail in future work.

IV. CONCLUSIONS AND OUTLOOK

Finally, we want to summarize our results and give a brief outlook. In this paper, we have presented detailed analytic formulas for the quark matter under rotation in the three-flavor NJL model and related topics have been investigated. In order to have a better understanding of the rotating system with finite density, we have also introduced the chemical potential. We studied the quark fields in cylindrical coordinates as well as investigated the effect of the rotation on the quark chiral condensate, quark spin polarization, and quark number susceptibility at finite temperature with or without finite chemical potential in this model. We found that the angular velocity plays a very crucial role in these topics, at low temperatures, small chemical potential, and small angular velocity the chiral symmetry is broken spontaneously, while at large enough angular velocity the chiral symmetry is restored. Our numerical analysis shows that the rotation suppresses the chiral condensation and enhances the first-order quark spin polarization, however for the second-order quark spin polarization and quark number susceptibility the effect is very complicated, which can be found to have a peak structure.

We have also explicitly computed these quantities in the rotation system in the presence of chemical potential. We found that the nonzero chemical potential affects and makes the chiral condensate, quark spin polarization, and quark number susceptibility have different behaviors. At very low temperatures, the chiral condensate

experiences a very rapid transition when angular velocity exceeds a certain value with zero chemical potential, while at large chemical potential this transition is suppressed and becomes a smooth crossover transition. It can be also observed that at very low temperatures, the quark number susceptibilities have two maxima, a plausible explanation for this phenomenon is that the rotational velocity serves as an effective chemical potential and exhibits a nontrivial behavior such that the competition between the chemical potential and angular velocity renders the quark number susceptibility to reach its maximum in such manner. In this paper, we especially considered the contributions from s quark and made some comparisons between u quark and s quark, and found that at small angular velocity the part played by mass in these phenomena is important, however, at sufficiently large angular velocity, the contributions played by different quarks to these phenomena are almost equal. In addition, we explored the chiral phase transition of rotating quark matter in the three-flavor NJL model, we observed that at very low temperatures there exist the chiral condensate experiences a very fast transition when angular velocity exceeds a certain value. Based on the interpretations made above, it would be possible to judge and forecast these phenomena of quark matter under rotation if we jointly take angular velocity, chemical potential, and temperature factors into consideration in the three-flavor NJL model. We expect these studies to play an important role in helping understand the properties of strongly interacting matter under rotation.

The theoretical interest in relativistic rotating systems is being revived in many different physical environments, the study also calls for more investigation on different aspects of the issue. For instance, the related effects of rotating fermions inside a cylindrical boundary [140], the investigation of a possible phase structure under rotation including the s quark, especially the exploration of those regions of the phase diagram that cannot be reached on the lattice yet. The NJL model describes only quarks and antiquarks and neglects the gluons, so it is also very worth extending the rotation system to the Polyakov extended Nambu–Jona-Lasinio (PNJL) model [141], which considers interactions between quarks and gluons, and the global rotation opens a new window to study the properties of QGP and a new direction in the study of heavy ion physics. This model will have a clearer picture considering the constraint from the experimental related to rotation conducted at numerous research facilities worldwide as the Brookhaven National Laboratory (BNL), the European Organization for Nuclear Research (CERN), and the GSI Helmholtz Centre for Heavy Ion Research (GSI), new insights are bound to result from upcoming experimental results and continued theoretical focus. It would be interesting to use the results obtained in this paper to investigate these topics which we leave to future studies.

ACKNOWLEDGMENTS

We specially thank Jinfeng Liao for the early involvement in the work and enlightening discussions and thank Hui Zhang, Akira Watanabe for discussions, corrections, and comments. We also thank Shengqin Feng and Yafei Shi for their encouragement and discussions. The work has been supported by the National Natural Science Foundation of China (NSFC) under Grant No. 11647174, No. 11875178, No. 11801311, the Key Laboratory of Quark and Lepton Physics Contracts under Grant No. QLPL201905, and the Science Research Foundation of China Three Gorges University under Grant No. KJ2015A007. A. H. acknowledges support by the NSF Grant No. PHY1913729 and by the U.S. Department of Energy, Office of Science, Office of Nuclear Physics, within the framework of the Beam Energy Scan Theory (BEST) Topical Collaboration. A. H. is also grateful to the Fundamental Research Funds for the Central Universities.

APPENDIX: BRIEF DESCRIPTION OF FERMIONS UNDER ROTATION

The properties of fermions under global rotation are relevant to a number of problems as discussed above, so it is important to choose an appropriate complete set of commuting operators in the cylindrical coordinates. In this section, we will start from the Dirac equation in the rotating frame, then we will derive the eigenvectors of the those complete set of commuting operators.

The general Lagrangian of the rotating fermions is written in the following way [16,30,92]

$$\mathcal{L}=\bar{\psi}[i\gamma^{\mu}\partial_{\mu}-m+(\gamma^{0})^{-1}((\vec{\omega}\times\vec{x})\cdot(-i\vec{\partial})+\vec{\omega}\cdot\vec{S}_{4\times4})]\psi, \tag{A1}$$

where ψ is the quark field, ω is the angular velocity and m is the bare quark mass matrix, as a result of rotation, we can see the Dirac operator includes the orbit-rotation coupling term and the spin-rotation coupling term, and we have defined

$$\vec{S}_{4\times4}=\frac{1}{2}\begin{pmatrix}\vec{\sigma} & 0\\ 0 & \vec{\sigma}\end{pmatrix}, \tag{A2}$$

whose z-component is related to the spin polarization of the quark. The corresponding Hamiltonian of Eq. (A1) in momentum space reads

$$\hat{\mathcal{H}}=\gamma^{0}(\vec{\gamma}\cdot\hat{\vec{p}}+m)-\vec{\omega}\cdot(\vec{x}\times\hat{\vec{p}}+\vec{S}_{4\times4})=\hat{\mathcal{H}}_{0}+\vec{\omega}\cdot\hat{\vec{J}}, \tag{A3}$$

here

$$\hat{\vec{J}} = \vec{x} \times \hat{\vec{p}} + \vec{S}_{4\times4}, \tag{A4}$$

and the first term is the contribution of the angular momentum, the second term is the contribution of the spin angular momentum.

Now considering the energy eigenvalue equation

$$\hat{\mathcal{H}}\psi = E\psi, \tag{A5}$$

here ψ is the four-component spinors and can be written in terms of two-component spinors as

$$\psi = \begin{pmatrix} \phi \\ \chi \end{pmatrix}, \tag{A6}$$

substituting the Hamiltonian above into the energy eigenvalue equation, then Eq. (A5) transforms simply as

$$\begin{cases} (E - m + \omega_z J_z)\phi = \vec{\sigma}.\hat{\vec{p}}\chi \\ (E + m + \omega_z J_z)\chi = \vec{\sigma}.\hat{\vec{p}}\phi \end{cases} \tag{A7}$$

here,

$$J_z = L_z + \frac{1}{2}\sum_z, \tag{A8}$$

which is the z-component of total angular momentum, then, we consider the z-component angular momentum eigenvalue equation

$$J_z\psi = \left(n + \frac{1}{2}\right)\psi, \tag{A9}$$

after some derivations, we can get the following equation

$$\left(E - m + \omega_z\left(n + \frac{1}{2}\right)\right)\left(E + m + \omega_z\left(n + \frac{1}{2}\right)\right)\phi = (\vec{\sigma}.\hat{\vec{p}})^2\phi, \tag{A10}$$

it is very convenient to make the transform Cartesian coordinate to the cylindrical coordinate. Here, the separation of variables method is applied and ϕ takes the form of

$$\phi = f(\theta)g(r)h(z), \tag{A11}$$

after solving the z-component angular momentum eigenvalue equation in Eq. (A9), the solution of $f(\theta)$ in the two-component spinors ϕ above has the form

$$f(\theta) = \begin{pmatrix} e^{in\theta} \\ e^{i(n+1)\theta} \end{pmatrix}, \tag{A12}$$

substituting Eq. (A12) into the Eq. (A10) after some tedious calculations, we find that $g(r)$ satisfies the Bessel-type equation as follows,

$$r^2\frac{\partial^2 g(r)}{\partial r^2} + r\frac{\partial g(r)}{\partial r} + (r^2p_t^2 - n^2)g(r) = 0, \tag{A13}$$

$$r^2\frac{\partial^2 g(r)}{\partial r^2} + r\frac{\partial g(r)}{\partial r} + (r^2p_t^2 - (n+1)^2)g(r) = 0, \tag{A14}$$

the solutions of Eqs. (A13) and (A14) have the following form, respectively,

$$g(r) = J_n(p_t r), J_{n+1}(p_t r), \tag{A15}$$

where J is the Bessel function. In order to commute with other operators, we must define the helicity operator, the general helicity operator has the following form

$$h_t = \gamma^5.\gamma^3\frac{\vec{\sum}.\vec{p}_t}{|\vec{p}_t|} = \frac{1}{i|\vec{p}_t|}\begin{pmatrix} 0 & -P_- & 0 & 0 \\ P_+ & 0 & 0 & 0 \\ 0 & 0 & 0 & P_- \\ 0 & 0 & -P_+ & 0 \end{pmatrix}, \tag{A16}$$

here, p_t is the transverse momentum, $P_+ = \hat{p}_x + i\hat{p}_y$, $P_- = \hat{p}_x - i\hat{p}_y$ and in cylindrical coordinates they have such forms

$$P_+ = -ie^{i\theta}\left(\frac{\partial}{\partial r} + i\frac{1}{r}\frac{\partial}{\partial\theta}\right), \tag{A17}$$

$$P_- = -ie^{-i\theta}\left(\frac{\partial}{\partial r} - i\frac{1}{r}\frac{\partial}{\partial\theta}\right), \tag{A18}$$

which like shift operators when act on the terms including angular momentum quantum number $e^{in\theta}J_n(p_t r)$, $e^{i(n+1)\theta}J_{n+1}(p_t r)$, respectively, they satisfy the following relationship

$$P_+e^{in\theta}J_n(p_t r) = ip_t e^{i(n+1)\theta}J_{n+1}(p_t r), \tag{A19}$$

$$P_-e^{i(n+1)\theta}J_{n+1}(p_t r) = -ip_t e^{in\theta}J_n(p_t r). \tag{A20}$$

Reconsidering the transverse helicity equation and the generalized orthogonality relation

$$h_t\psi = s\psi, \tag{A21}$$

$$\sum_{n=-\infty}^{\infty}\psi^\dagger\psi = 1, \tag{A22}$$

here, $s = \pm1$ represent the transverse helicity, the solutions of the positive energy eigenvalues are obtained as follows

$$u = \frac{1}{\sqrt{2}} \begin{pmatrix} e^{ip_z z} e^{in\theta} J_n(p_t r) \\ s e^{ip_z z} e^{i(n+1)\theta} J_{n+1}(p_t r) \\ e^{ip_z z} e^{in\theta} J_n(p_t r) \\ s e^{ip_z z} e^{i(n+1)\theta} J_{n+1}(p_t r) \end{pmatrix}, \tag{A23}$$

where u is a four-component spinor that must satisfy the Dirac equation

$$(i\gamma^\mu \partial_\mu - m)u = 0, \tag{A24}$$

substituting u into the Dirac equation gives

$$\begin{pmatrix} E - m & -\sigma.p \\ \sigma.p & -E - m \end{pmatrix} \begin{pmatrix} c_A u_A \\ c_B u_B \end{pmatrix} = 0, \tag{A25}$$

here u_A, u_B are two-component spinors and c_A, c_B are normalization constants, after some calculations we get

$$c_B u_B = c_A \begin{pmatrix} \frac{(p_z - i s p_t)}{E+m} e^{ip_z z} e^{in\theta} J_n(p_t r) \\ \frac{(-s p_z + i p_t)}{E+m} e^{ip_z z} e^{i(n+1)\theta} J_{n+1}(p_t r) \end{pmatrix}, \tag{A26}$$

imposing the generalized completeness relation

$$\sum_{n=-\infty}^{\infty} u^\dagger u = 1, \tag{A27}$$

these constant factors can be determined and finally, we obtain the positive energy particle solutions with positive and negative helicity in the Dirac representation, which take the following explicit form

$$u = \frac{1}{2}\sqrt{\frac{E+m}{E}} \begin{pmatrix} e^{ip_z z} e^{in\theta} J_n(p_t r) \\ s e^{ip_z z} e^{i(n+1)\theta} J_{n+1}(p_t r) \\ \frac{p_z - i s p_t}{E+m} e^{ip_z z} e^{in\theta} J_n(p_t r) \\ \frac{-s p_z + i p_t}{E+m} e^{ip_z z} e^{i(n+1)\theta} J_{n+1}(p_t r) \end{pmatrix}, \tag{A28}$$

in exactly the same way, the negative-energy antiparticle solutions are listed below

$$v = \frac{1}{2}\sqrt{\frac{E+m}{E}} \begin{pmatrix} \frac{p_z - i s p_t}{E+m} e^{-ip_z z} e^{in\theta} J_n(p_t r) \\ \frac{-s p_z + i p_t}{E+m} e^{-ip_z z} e^{i(n+1)\theta} J_{n+1}(p_t r) \\ e^{-ip_z z} e^{in\theta} J_n(p_t r) \\ -s e^{-ip_z z} e^{i(n+1)\theta} J_{n+1}(p_t r) \end{pmatrix}. \tag{A29}$$

[1] D. Kharzeev and A. Zhitnitsky, Nucl. Phys. **A797**, 67 (2007).
[2] D. T. Son and P. Surowka, Phys. Rev. Lett. **103**, 191601 (2009).
[3] D. E. Kharzeev and D. T. Son, Phys. Rev. Lett. **106**, 062301 (2011).
[4] Y. Jiang, X. G. Huang, and J. Liao, Phys. Rev. D **92**, 071501 (2015).
[5] D. E. Kharzeev, J. Liao, S. A. Voloshin, and G. Wang, Prog. Part. Nucl. Phys. **88**, 1 (2016).
[6] L. P. Csernai, V. K. Magas, and D. J. Wang, Phys. Rev. C **87**, 034906 (2013).
[7] F. Becattini, G. Inghirami, V. Rolando, A. Beraudo, L. Del Zanna, A. De Pace, M. Nardi, G. Pagliara, and V. Chandra, Eur. Phys. J. C **75**, 406 (2015).
[8] Y. Jiang, Z. W. Lin, and J. Liao, Phys. Rev. C **94**, 044910 (2016); **95**, 049904(E) (2017).
[9] S. Shi, K. Li, and J. Liao, Phys. Lett. B **788**, 409 (2019).
[10] W. T. Deng and X. G. Huang, Phys. Rev. C **93**, 064907 (2016).
[11] L. G. Pang, H. Petersen, Q. Wang, and X. N. Wang, Phys. Rev. Lett. **117**, 192301 (2016).
[12] L. Adamczyk *et al.* (STAR Collaboration), Nature (London) **548**, 62 (2017).
[13] F. Becattini, I. Karpenko, M. Lisa, I. Upsal, and S. Voloshin, Phys. Rev. C **95**, 054902 (2017).
[14] X. L. Xia, H. Li, Z. B. Tang, and Q. Wang, Phys. Rev. C **98**, 024905 (2018).
[15] Hui Zhang, Defu Hou, and Jinfeng Liao, Chin. Phys. C **44**, 111001 (2020).
[16] A. L. Fetter, Rev. Mod. Phys. **81**, 647 (2009).
[17] M. Urban and P. Schuck, Phys. Rev. A **78**, 011601 (2008).
[18] M. Iskin and E. Tiesinga, Phys. Rev. A **79**, 053621 (2009).
[19] R. Takahashi, M. Matsuo, M. Ono, K. Harii, H. Chudo, S. Okayasu, J. Ieda, S. Takahashi, S. Maekawa, and E. Saitoh, Nat. Phys. **12**, 52 (2016).
[20] J. Gooth *et al.*, Nature (London) **547**, 324 (2017).
[21] A. Vilenkin, Phys. Lett. **80B**, 150 (1978).
[22] A. Vilenkin, Phys. Rev. D **20**, 1807 (1979).
[23] A. Vilenkin, Phys. Rev. D **21**, 2260 (1980).
[24] M. Kaminski, C. F. Uhlemann, M. Bleicher, and J. Schaffner-Bielich, Phys. Lett. B **760**, 170 (2016).
[25] N. Yamamoto, Phys. Rev. D **93**, 065017 (2016).
[26] E. Shaverin and A. Yarom, Nucl. Phys. **B928**, 268 (2018).
[27] A. L. Watts *et al.*, Rev. Mod. Phys. **88**, 021001 (2016).
[28] I. A. Grenier and A. K. Harding, C.R. Phys. **16**, 641 (2015).
[29] E. Berti, F. White, A. Maniopoulou, and M. Bruni, Mon. Not. R. Astron. Soc. **358**, 923 (2005).

[30] A. Yamamoto and Y. Hirono, Phys. Rev. Lett. **111**, 081601 (2013).
[31] Z. T. Liang and X. N. Wang, Phys. Rev. Lett. **94**, 102301 (2005); **96**, 039901(E) (2006).
[32] Sergei A. Voloshin, arXiv:nucl-th/0410089.
[33] F. Becattini, F. Piccinini, and J. Rizzo, Phys. Rev. C **77**, 024906 (2008).
[34] Z. T. Liang and X. N. Wang, Phys. Rev. Lett. **94**, 102301 (2005); **96**, 039901(E) (2006).
[35] X. G. Huang, P. Huovinen, and X. N. Wang, Phys. Rev. C **84**, 054910 (2011).
[36] X. G. Huang, Rep. Prog. Phys. **79**, 076302 (2016).
[37] F. Becattini and F. Piccinini, Ann. Phys. (Amsterdam) **323**, 2452 (2008).
[38] F. Becattini, V. Chandra, L. Del Zanna, and E. Grossi, Ann. Phys. (Amsterdam) **338**, 32 (2013).
[39] F. Becattini, G. Inghirami, V. Rolando, A. Beraudo, L. Del Zanna, A. De Pace, M. Nardi, G. Pagliara, and V. Chandra, Eur. Phys. J. C **75**, 406 (2015).
[40] A. Aristova, D. Frenklakh, A. Gorsky, and D. Kharzeev, J. High Energy Phys. 10 (2016) 029.
[41] W. T. Deng and X. G. Huang, Phys. Rev. C **93**, 064907 (2016).
[42] Shu Ebihara, Kenji Fukushima, and Kazuya Mameda, Phys. Lett. B **764**, 94 (2017).
[43] L. Adamczyk *et al.* (STAR Collaboration), Nature (London) **548**, 62 (2017).
[44] J. Adam *et al.* (STAR Collaboration), Phys. Rev. C **98**, 014910 (2018).
[45] S. Acharya *et al.* (ALICE Collaboration), Phys. Rev. C **101**, 044611 (2020).
[46] Y. Tsue, J. da Providência, C. Providência, M. Yamamura, and H. Bohr, Prog. Theor. Exp. Phys. **2013**, 103D01 (2013).
[47] Y. Tsue, J. da Providência, C. Providência, M. Yamamura, and H. Bohr, Prog. Theor. Exp. Phys. **2015**, 103D02 (2015).
[48] Y. Tsue, J. da Providência, C. Providência, M. Yamamura, and H. Bohr, Prog. Theor. Exp. Phys. **2015**, 103D01 (2015).
[49] H. Matsuoka, Y. Tsue, J. da Providência, C. Providência, M. Yamamura, and H. Bohr, Prog. Theor. Exp. Phys. **2016**, 053D02 (2016).
[50] H. Matsuoka, Y. Tsue, J. da Providência, and M. Yamamura, Phys. Rev. D **95**, 054025 (2017).
[51] X. G. Huang, J. Liao, Q. Wang, and X. L. Xia, Lect. Notes Phys. **987**, 281 (2021).
[52] F. Becattini and M. A. Lisa, Annu. Rev. Nucl. Part. Sci. **70**, 395 (2020).
[53] Yu Guo, Jinfeng Liao, Enke Wang, Hongxi Xing, and Hui Zhang, Phys. Rev. C **104**, L041902 (2021).
[54] S. Jeon and V. Koch, Event by event fluctuations, in *Quark Gluon Plasma*, edited by R. C. Hwa and X. N. Wang (World Scientific, Singapore, 2004), pp. 430–490.
[55] V. Koch, arXiv:0810.2520.
[56] A. Bzdak, V. Koch, and J. Liao, Phys. Rev. C **81**, 031901 (2010).
[57] X.-F. Luo (STAR Collaboration), J. Phys. Conf. Ser. **316**, 012003 (2011).
[58] S. Gupta, X. Luo, B. Mohanty, H. G. Ritter, and N. Xu, Science **332**, 1525 (2011).
[59] A. Bzdak, V. Koch, and J. Liao, Lect. Notes Phys. **871**, 503 (2013).
[60] A. Bazavov *et al.*, Phys. Rev. Lett. **109**, 192302 (2012).
[61] X. F. Luo, B. Mohanty, H. G. Ritter, and N. Xu, Phys. At. Nucl. **75**, 676 (2012).
[62] X. Luo, J. Xu, B. Mohanty, and N. Xu, J. Phys. G **40**, 105104 (2013).
[63] X. Luo (STAR Collaboration), Nucl. Phys. **A904-905**, 911c (2013).
[64] Shuzhe Shi and Jinfeng Liao, J. High Energy Phys. 06 (2013) 104.
[65] R. V. Gavai and S. Gupta, Phys. Rev. D **68** (2003) 034506.
[66] R. V. Gavai and S. Gupta, Phys. Rev. D **71** (2005) 114014.
[67] S. Gupta, N. Karthik, and P. Majumdar, Phys. Rev. D **90**, 034001 (2014).
[68] L. Adamczyk *et al.* (STAR Collaboration), Phys. Rev. Lett. **112**, 032302 (2014).
[69] L. Adamczyk *et al.* (STAR Collaboration), Phys. Rev. Lett. **113**, 092301 (2014).
[70] X. Luo, EPJ Web Conf. **141**, 04001 (2017).
[71] R. Gavai and S. Gupta, Phys. Rev. D **73**, 014004 (2006).
[72] S. Borsanyi, Z. Fodor, S. Katz, S. Krieg, C. Ratti, and K. Szabo, Phys. Rev. Lett. **111**, 062005 (2013).
[73] S. Borsanyi, Nucl. Phys. **A904-905**, 270c (2013).
[74] R. Bellwied, S. Borsanyi, Z. Fodor, S. Katz, A. Pasztor, C. Ratti, and K. Szabo, Phys. Rev. D **92**, 114505 (2015).
[75] H. T. Ding, S. Mukherjee, H. Ohno, P. Petreczky, and H. P. Schadler, Phys. Rev. D **92**, 074043 (2015).
[76] T. Kunihiro, Phys. Lett. B **271**, 395 (1991).
[77] H. Fujii and M. Ohtani, Phys. Rev. D **70**, 014016 (2004).
[78] Y. Hatta and T. Ikeda, Phys. Rev. D **67**, 014028 (2003).
[79] B. J. Schaefer and J. Wambach, Phys. Rev. D **75**, 085015 (2007).
[80] A. R. Bodmer, Phys. Rev. D **4**, 1601 (1971).
[81] E. Witten, Phys. Rev. D **30**, 272 (1984).
[82] C. Alcock, E. Farhi, and A. V. Olinto, Astrophys. J. **310**, 261 (1986).
[83] C. Alcock and A. V. Olinto, Annu. Rev. Nucl. Part. Sci. **38**, 161 (1988).
[84] J. Madsen, Lect. Notes Phys. **516**, 162 (1999).
[85] N. K. Glendenning and F. Weber, Astrophys. J. **400**, 647 (1992).
[86] N. K. Glendenning, Ch. Kettner, and F. Weber, Astrophys. J. **450**, 253 (1995).
[87] N. K. Glendenning, Ch. Kettner, and F. Weber, Phys. Rev. Lett. **74**, 3519 (1995).
[88] H. Terazawa, INS, University of Tokyo Report No. INS-Report-338, 1979.
[89] H. Terazawa, J. Phys. Soc. Jpn. **58**, 3555 (1989).
[90] H. Terazawa, J. Phys. Soc. Jpn. **58**, 4388 (1989).
[91] H. Terazawa, J. Phys. Soc. Jpn. **59**, 1199 (1990).
[92] Y. Jiang and J. Liao, Phys. Rev. Lett. **117**, 192302 (2016).
[93] M. Buballa, Phys. Rep. **407**, 205 (2005).
[94] Renan Cãmara Pereiraa, João Moreirab, and Pedro Costac, Eur. Phys. J. A **56**, 214 (2020).
[95] T. Hatsuda and T. Kunihiro, Phys. Rep. **247**, 221 (1994).
[96] S. P. Klevansky, Rev. Mod. Phys. **64**, 649 (1992).

[97] B. Hiller, J. Moreira, A. A. Osipov, and A. H. Blin, Phys. Rev. D **81**, 116005 (2010).
[98] A. Bhattacharyya, P. Deb, S. K. Ghosh, and R. Ray, Phys. Rev. D **82**, 014021 (2010).
[99] J. I. Kapusta, *Finite Temperature Field Theory* (Cambridge University Press, Cambridge, England, 1989).
[100] F. Becattinia and F. Piccinini, Ann. Phys. (Amsterdam) **323**, 2452 (2008).
[101] R. V. Gavai and S. Gupta, Phys. Rev. D **68**, 034506 (2003).
[102] R. V. Gavai and S. Gupta, Phys. Rev. D **72**, 054006 (2005).
[103] R. V. Gavai and S. Gupta, Phys. Rev. D **71**, 114014 (2005).
[104] C. R. Allton, M. Döring, S. Ejiri, S. J. Hands, O. Kaczmarek, F. Karsch, E. Laermann, and K. Redlich, Phys. Rev. D **71**, 054508 (2005).
[105] M. Cheng *et al.*, Phys. Rev. D **79**, 074505 (2009).
[106] S. Borsányi, Z. Fodor, S. D. Katz, S. Krieg, C. Ratti, and K. Szabó, J. High Energy Phys. 01 (2012) 138.
[107] A. Bazavov *et al.* (HotQCD Collaboration), Phys. Rev. D **86**, 034509 (2012).
[108] H. L. Chen, K. Fukushima, X. G. Huang, and K. Mameda, Phys. Rev. D **93**, 104052 (2016).
[109] S. Ebihara, K. Fukushima, and K. Mameda, Phys. Lett. B **764**, 94 (2017).
[110] M. N. Chernodub and S. Gongyo, J. High Energy Phys. 01 (2017) 136.
[111] M. N. Chernodub and S. Gongyo, Phys. Rev. D **95**, 096006 (2017).
[112] M. N. Chernodub, Phys. Rev. D **103**, 054027 (2021).
[113] Xinyang Wang, Minghua Wei, Zhibin Li, and Mei Huang, Phys. Rev. D **99**, 016018 (2019).
[114] H. Kohyama, D. Kimura, and T. Inagaki, Nucl. Phys. **B906**, 524 (2016).
[115] V. V. Braguta, A. Yu. Kotov, D. D. Kuznedelev, and A. A. Roenko, Phys. Rev. D **103**, 094515 (2021).
[116] V. V. Braguta, A. Yu. Kotov, D. D. Kuznedelev, and A. A. Roenko, Proc. Sci., LATTICE2021 (**2022**) 125.
[117] P. de Forcrand, Proc. Sci., LAT2009 (**2009**) 010, arXiv:1005.0539.
[118] H. Kohyama, D. Kimura, and T. Inagaki, Nucl. Phys. **B896**, 682 (2015).
[119] C. D. Roberts and A. G. Williams, Prog. Part. Nucl. Phys. **33**, 477 (1994).
[120] R. Alkofer and L. Von Smekal, Phys. Rep. **353**, 281 (2001).
[121] C. S. Fischer, J. Phys. G **32**, R253 (2006).
[122] I. C. Cloët and C. D. Roberts, Prog. Part. Nucl. Phys. **77**, 1 (2014).
[123] T. M. Schwarz, S. P. Klevansky, and G. Papp, Phys. Rev. C **60**, 055205 (1999).
[124] P. Zhuang, M. Huang, and Z. Yang, Phys. Rev. C **62**, 054901 (2000).
[125] J. W. Chen, J. Deng, and L. Labun, Phys. Rev. D **92**, 054019 (2015).
[126] J. W. Chen, J. Deng, H. Kohyama, and L. Labun, Phys. Rev. D **93**, 034037 (2016).
[127] W. Fan, X. Luo, and H.-S. Zong, Int. J. Mod. Phys. A **32**, 1750061 (2017).
[128] W. Fan, X. Luo, and H. Zong, Chin. Phys. C **43**, 033103 (2019).
[129] W. J. Fu and Y. L. Wu, Phys. Rev. D **82**, 074013 (2010).
[130] E. S. Bowman and J. I. Kapusta, Phys. Rev. C **79**, 015202 (2009).
[131] H. Mao, J. Jin, and M. Huang, J. Phys. G **37**, 035001 (2010).
[132] B. J. Schaefer and M. Wagner, Phys. Rev. D **85**, 034027 (2012).
[133] B. J. Schaefer and M. Wagner, Central Eur. J. Phys. **10**, 1326 (2012).
[134] S. X. Qin, L. Chang, H. Chen, Y.-X. Liu, and C. D. Roberts, Phys. Rev. Lett. **106**, 172301 (2011).
[135] J. Luecker, C. S. Fischer, L. Fister, and J. M. Pawlowski, Proc. Sci., CPOD2013 (**2013**) 057, arXiv:1308.4509, https://pos.sissa.it/185/057/pdf.
[136] W. J. Fu, J. M. Pawlowski, F. Rennecke, and B.-J. Schaefer, Phys. Rev. D **94**, 116020 (2016).
[137] Luis A. H. Mamani, Cesar V. Flores, and Vilson T. Zanchin, Phys. Rev. D **102**, 066006 (2020).
[138] Juan M. Torres-Rincon and Joerg Aichelin, Phys. Rev. C **96**, 045205 (2017).
[139] J. N. Guenther, Eur. Phys. J. A **57**, 136 (2021).
[140] Victor E. Ambrus and Elizabeth Winstanley, Phys. Rev. D **93**, 104014 (2016).
[141] C. Ratti, M. A. Thaler, and W. Weise, Phys. Rev. D **73**, 014019 (2006).